

## ORIGINAL ARTICLE OPEN ACCESS

# *Pseudomonas syringae* pv. *tabaci* 6605 Requires Seven Type III Effectors to Infect *Nicotiana benthamiana*

Kana Kuroe | Takafumi Nishimura | Sachi Kashihara | Nanami Sakata  | Mikihiro Yamamoto | Yoshiteru Noutoshi  | Kazuhiro Toyoda  | Yuki Ichinose  | Hidenori Matsui 

Graduate School of Environmental, Life, Natural Science and Technology, Okayama University, Kita-ku, Okayama, Japan

**Correspondence:** Hidenori Matsui ([hmatsui@okayama-u.ac.jp](mailto:hmatsui@okayama-u.ac.jp))**Received:** 11 March 2025 | **Revised:** 18 April 2025 | **Accepted:** 22 April 2025**Funding:** This work was supported in part by Grants-in-Aid for Scientific Research (H.M., 22K05653; Y.I., 23K23613) from the Ministry of Education, Culture, Sports, Science and Technology of Japan.**Keywords:** poly T3E mutant | type III effector | type III secretion system

## ABSTRACT

Type III effectors (T3Es), virulence factors injected into plant cells via the type III secretion system (T3SS), play essential roles in the infection of host plants. *Pseudomonas syringae* pv. *tabaci* 6605 (Pta 6605) is the causal agent of wildfire disease in tobacco and harbours at least 22 T3Es in its genome. However, the specific T3Es required by Pta 6605 to infect *Nicotiana benthamiana* remain unidentified. In this study, we investigated the T3Es that contribute to Pta 6605 infection of *N. benthamiana*. We constructed Pta 6605 poly-T3E-deficient mutants (Pta DxE) and inoculated them into *N. benthamiana*. Flood assay, which mimics natural opening-based entry, showed that mutant strains lacking 14–22 T3Es, namely, Pta D14E–D22E mutants, exhibited reduced disease symptoms. By contrast, infiltration inoculation, which involves direct injection into leaves, showed that the Pta D14E to Pta D20E mutants developed disease symptoms. Notably, the Pta D20E, containing AvrE1 and HopM1, induced weak but observable symptoms upon infiltration inoculation. Conversely, no symptoms were observed in either the flood assay or infiltration inoculation for Pta D21E and Pta D22E. Taken together, these findings indicate that the many T3Es such as AvrPto4/AvrPtoB, HopW1/HopAE1, and HopM1/AvrE1 in Pta 6605 collectively contribute to invasion through natural openings and symptom development in *N. benthamiana*. This study provides the basis for understanding virulence in the host by identifying the minimum T3E repertoire required by Pta 6605 to infect *N. benthamiana*.

## 1 | Introduction

Plant-pathogenic bacteria use an array of virulence factors to establish infection in their host plants. Type III effectors (T3Es) are key virulence factors for successful infection. The conserved type III secretion system (T3SS) mediates the secretion of T3Es, which facilitate disease progression (Büttner 2016). For example, T3Es inhibit downstream immune signalling pathways and suppress plant immune responses by targeting pattern recognition receptor complexes (Coburn et al. 2007; Speth et al. 2007; Zhou and Chai 2008; Khan et al. 2018). T3Es also regulate host metabolism, hormonal

signalling, and stomatal immunity (Yang et al. 2017; Melotto et al. 2024).

*Pseudomonas syringae*, a gram-negative bacterium, infects a wide range of plant species (Xin et al. 2018). *Pseudomonas* species harbour 20 to 50 T3Es in their genomes. The T3E repertoire varies among individual strains (Dillon et al. 2019). T3E orthologues trigger different responses in the same host. A previous study investigated the ability of AvrPto orthologues to induce cell death in *Nicotiana benthamiana* and found that AvrPto and related orthologues from *P. syringae* pv. *tomato* (Pto) DC3000 induce a Pto-dependent hypersensitive

This is an open access article under the terms of the [Creative Commons Attribution-NonCommercial](https://creativecommons.org/licenses/by-nc/4.0/) License, which permits use, distribution and reproduction in any medium, provided the original work is properly cited and is not used for commercial purposes.

© 2025 The Author(s). *Molecular Plant Pathology* published by British Society for Plant Pathology and John Wiley & Sons Ltd.

response, whereas distantly related orthologues do not (Baltrus et al. 2011). Additionally, the virulence and avirulence functions of AvrPto are determined by specific amino acid substitutions. These findings highlight the complex functions of T3Es and underscore the need for further investigation to fully understand their roles in the interactions between host and pathogen. Various approaches have been developed to systematically investigate T3E functions. For example, poly-T3E gene deletion strains, such as Pto DC3000, have been generated (Cunnac et al. 2011; Wei et al. 2018). Alternatively, a system for evaluating T3E function has been constructed by introducing the T3SS system using cosmid pLN18 and T3Es into *Pseudomonas fluorescens* (Oh et al. 2010). These approaches enable the dissection of complex interactions between T3Es and host plant immunity systems, providing insights into the role of multiple effectors (Xin et al. 2016; Chakravarthy et al. 2018; Roussin-Léveillé et al. 2022).

Pto DC3000 can infect *Arabidopsis* and tomato, and its *hopQ1-1*-deficient strain can infect *N. benthamiana* (Wei et al. 2007). Furthermore, a minimal set of T3Es (AvrE1, HopM1, HopE1, AvrPtoB, HopG1, HopAA1-1, and HopAM1) secreted by Pto DC3000 is essential for *N. benthamiana* infection (Cunnac et al. 2011). However, *P. syringae* pv. *tabaci* (Pta) 11528 and *P. syringae* pv. *syringae* (Pss) B728a can infect *N. benthamiana* even without HopE1, HopG1, and HopAM1 (Studholme et al. 2009). This finding suggests that these strains use alternative effectors or mechanisms, which are not yet characterised, to suppress plant immunity and cause disease (Cunnac et al. 2011).

Pta 6605 causes wildfire disease with severe symptoms in *N. benthamiana* (Kashihara et al. 2022). Genomic analyses predict that Pta 6605 harbours at least 22 distinct T3Es (Matsui et al. 2021). However, the T3E repertoire required for infection of *N. benthamiana* by Pta 6605 remains unclear, and many of their functions are still unknown. Thus, this study was aimed at identifying the minimal T3E repertoire required by Pta 6605 to infect *N. benthamiana* and elucidate the underlying virulence mechanisms. Single and polyT3E-deficient mutant strains of Pta 6605 were generated, and the contribution of Pta T3Es to virulence was assessed. We have established a basis for understanding the role of T3Es in the infection of host plants by identifying the minimum T3E repertoire required by Pta 6605 to infect *N. benthamiana* through natural openings.

## 2 | Results

### 2.1 | Virulence of Single-Locus T3E Mutants of Pta in *N. benthamiana*

Pta 6605 is a pathogenic bacterium in *N. benthamiana* (Kashihara et al. 2022). To identify the key T3Es required by Pta 6605 to infect *N. benthamiana*, we performed inoculation assays using a series of single-locus T3E mutants. These experiments involved previously generated Pta T3E single-locus deletion mutants and a newly constructed Pta  $\Delta$ *hopF1* mutant (Kashihara et al. 2022; Table 1). We employed a flood inoculation assay system mimicking natural infection to assess bacterial entry through natural openings. In addition, symptom

onset was monitored at three levels: (1) severe; (2) half diseased; and (3) healthy. All single-locus T3E deletion mutants of Pta 6605 induced severe disease symptoms comparable to those induced by Pta wild type (WT) in *N. benthamiana* (Figure 1a,b). These findings indicate that the loss of a single T3E locus in Pta 6605 contributes little to its virulence to *N. benthamiana*.

### 2.2 | Pta Poly-T3E Mutants and Their Virulence

First, we focused on AvrPto4 and AvrPtoB, the two main effectors targeting pattern-triggered immunity (PTI), and investigated whether the Pta  $\Delta$ *avrPto4* $\Delta$ *avrPtoB* (D2E) mutant strain, similar to Pto DC3000, which infects tomato plants (Lin and Martin 2005), shows reduced virulence. Compared with Pta WT, the Pta D2E mutant showed an approximately 20% higher ratio of class 1–2 disease index, indicating that Pta D2E has slightly reduced symptoms (Figure 2a,b). However, no significant difference was observed in bacterial population between the Pta D2E mutant and Pta WT (Figure 2c). Considering the limited effect of the Pta D2E strain on symptom development, we constructed poly-T3E deletion mutants based on the Pta D2E mutant through homologous recombination with the pK18*mob-sacBN* vector to delete either the entire or partial T3E gene loci. In constructing poly-T3E deletion mutants, we performed transient overexpression assays of individual T3Es in *N. benthamiana* through agroinfiltration (Figure S1a,b). The results indicated that the transient expression of AvrE1, HopAE1, HopM1, HopT1, and HopW1 induced cell death, whereas the expression of HopAR1 resulted in chlorosis-like symptoms. Based on these observations, the deletion order was determined by initially targeting those T3Es that did not induce cell death in the transient expression assay. Following the naming convention used for Pto DC3000 (Wei et al. 2015), we designated the generated poly-T3E mutant ‘Pta DxE’, where ‘x’ denotes the number of T3Es deleted (Table 1).

First, we examined the motility of the Pta DxE mutants. This is because a decrease in motility in Pta 6605 leads to a decrease in virulence (Ichinose et al. 2003). We found no significant difference in motility between Pta DxE and Pta WT (Figure S2). This result indicates that motility is not affected by T3E deletions. We also performed in vitro bacterial growth assays using OD-based measurements. The results confirmed that the growth rates of all strains were comparable to that of Pta WT (Figure S3).

### 2.3 | Attenuated Symptom Development in Flood Assay of Pta D14E to D22E Mutants

To assess the virulence of the poly-T3E mutants, we inoculated *N. benthamiana* using a flood assay (Figure 2a). The Pta D3E to Pta D13E mutants induced disease symptoms at levels comparable to those induced by Pta D2E. Plants inoculated with Pta D14E to Pta D22E displayed remarkably reduced symptom development compared to those inoculated with Pta WT. To quantify symptom severity and determine a disease index, we measured and classified symptom development at 6 days post-inoculation (dpi) with three levels (Figure 2b). The Pta D14E mutant reduced disease symptoms, whereas the Pta D16E mutant

**TABLE 1** | Bacterial strains and plasmids.

Bacterial strain/plasmid	Relevant characteristics	References or source
<i>Escherichia coli</i>		
DH5 $\alpha$	$F^- \lambda^- \phi 80dLacZ \Delta M15 \Delta(lacZYA-argF)U169 recA1endA1 hsdR17(rK-mK+) supE44 thi-1 gyrA relA1$	TaKaRa
S17-1	<i>thi pro hsdR hsdR hsdM<sup>+</sup>recA(chr::RP4-2-Tc::Mu-Km::Tn7)</i>	Schäfer et al. (1994)
<i>P. syringae</i> pv. <i>tabaci</i> (Pta)		
Isolate 6605	Wild type isolated from tobacco, Nal <sup>r</sup>	Shimizu et al. (2003)
Pta $\Delta hrcC$	Isolate 6605 $\Delta$ Pta6605_RS21955, Nal <sup>r</sup>	Marutani et al. (2005)
Pta $\Delta avrE1$	Isolate 6605 $\Delta$ Pta6605_RS22015, Nal <sup>r</sup>	Kashihara et al. (2022)
Pta $\Delta avrPto4$	Isolate 6605, $\Delta$ Pta6605_RS26865, Nal <sup>r</sup>	Kashihara et al. (2022)
Pta $\Delta avrPtoB$	Isolate 6605 $\Delta$ Pta6605_RS12680, Nal <sup>r</sup>	Kashihara et al. (2022)
Pta $\Delta hopAE1$	Isolate 6605 $\Delta$ Pta6605_RS04955, Nal <sup>r</sup>	Kashihara et al. (2022)
Pta $\Delta hopAG1\Delta hopAH1\Delta hopAI1$	Isolate 6605 $\Delta$ RS0109770 (old acc.num.), $\Delta$ Pta6605_RS24195, $\Delta$ Pta6605_RS24190, Nal <sup>r</sup>	Kashihara et al. (2022)
Pta $\Delta hopAH2$	Isolate 6605 $\Delta$ Pta6605_RS11715, Nal <sup>r</sup>	Kashihara et al. (2022)
Pta $\Delta hopAR1$	Isolate 6605, $\Delta$ Pta6605_RS26885, Nal <sup>r</sup>	Kashihara et al. (2022)
Pta $\Delta hopAS1$	Isolate 6605, $\Delta$ Pta6605_RS25775, Nal <sup>r</sup>	Kashihara et al. (2022)
Pta $\Delta hopAZ1$	Isolate 6605, $\Delta$ Pta6605_RS18960, Nal <sup>r</sup>	Kashihara et al. (2022)
Pta $\Delta hopBD1$	Isolate 6605, $\Delta$ Pta6605_RS13890, Nal <sup>r</sup>	Kashihara et al. (2022)
Pta $\Delta hopE1$	Isolate 6605, $\Delta$ Pta6605_RS18765, Nal <sup>r</sup>	Kashihara et al. (2022)
Pta $\Delta hopF1$	Isolate 6605, $\Delta$ Pta6605_RS20695, Nal <sup>r</sup>	This study
Pta $\Delta hopI1$	Isolate 6605, $\Delta$ Pta6605_RS04760, Nal <sup>r</sup>	Kashihara et al. (2022)
Pta $\Delta hopM1-shcE$	Isolate 6605, $\Delta$ Pta6605_RS22025 $\Delta$ Pta6605_RS22020, Nal <sup>r</sup>	Kashihara et al. (2022)
Pta $\Delta hopOI1\Delta hopT1$	Isolate 6605, $\Delta$ Pta6605_RS20735, $\Delta$ Pta6605_RS20740, Nal <sup>r</sup>	Kashihara et al. (2022)
Pta $\Delta hopR1$	Isolate 6605, $\Delta$ Pta6605_RS00920, Nal <sup>r</sup>	Kashihara et al. (2022)
Pta $\Delta hopV1$	Isolate 6605, $\Delta$ Pta6605_RS12945, Nal <sup>r</sup>	Kashihara et al. (2022)
Pta $\Delta hopW1$	Isolate 6605, $\Delta$ Pta6605_RS13905, Nal <sup>r</sup>	Kashihara et al. (2022)
Pta $\Delta hopX1$	Isolate 6605, $\Delta$ Pta6605_RS28265, Nal <sup>r</sup>	Kashihara et al. (2022)
Pta D2E	Pta $\Delta avrPto4\Delta avrPtoB$ , Nal <sup>r</sup>	This study
Pta D3E	Pta D2E, $\Delta hopR1$ , Nal <sup>r</sup>	This study
Pta D4E	Pta D3E, $\Delta hopAH2$ , Nal <sup>r</sup>	This study
Pta D5E	Pta D4E, $\Delta hopI1$ , Nal <sup>r</sup>	This study
Pta D6E	Pta D5E, $\Delta hopV1$ , Nal <sup>r</sup>	This study
Pta D7E	Pta D6E, $\Delta hopBD1$ , Nal <sup>r</sup>	This study
Pta D8E	Pta D7E, $\Delta hopE1$ , Nal <sup>r</sup>	This study
Pta D9E	Pta D8E, $\Delta hopX1$ , Nal <sup>r</sup>	This study
Pta D12E	Pta D9E, $\Delta hopAG1\Delta hopAI1\Delta hopAH1$ , Nal <sup>r</sup>	This study
Pta D13E	Pta D12E, $\Delta hopAS1$ , Nal <sup>r</sup>	This study
Pta D14E	Pta D13E, $\Delta hopAR1$ , Nal <sup>r</sup>	This study

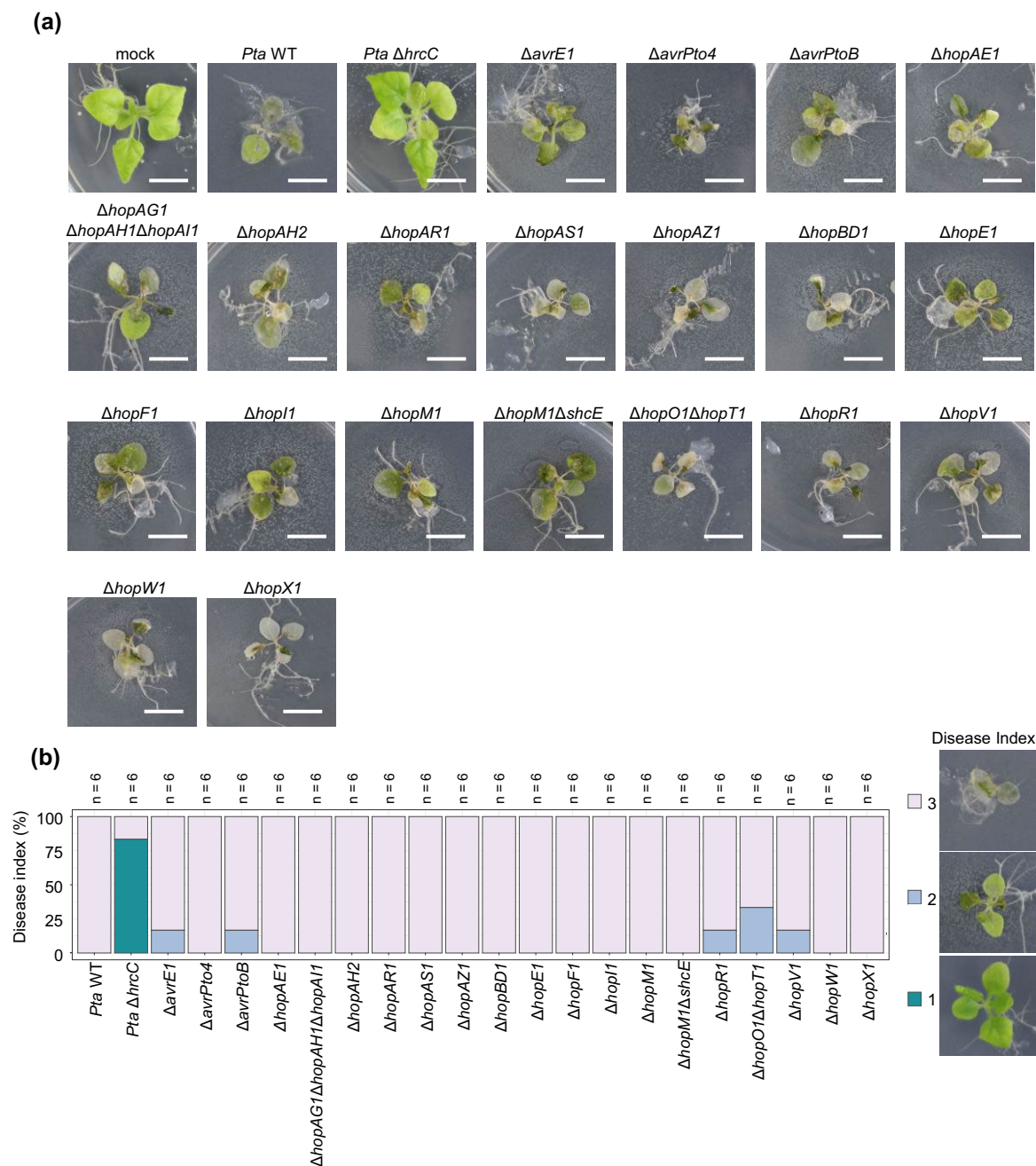
(Continues)

TABLE 1 | (Continued)

Bacterial strain/plasmid	Relevant characteristics	References or source
Pta D15E	Pta D14E, $\Delta$ hopF1, Nal <sup>r</sup>	This study
Pta D16E	Pta D15E, $\Delta$ hopAZI, Nal <sup>r</sup>	This study
Pta D17E	Pta D16E, $\Delta$ hopW1, Nal <sup>r</sup>	This study
Pta D18E	Pta D17E, $\Delta$ hopAE1, Nal <sup>r</sup>	This study
Pta D20E	Pta D18E, $\Delta$ hopT1 $\Delta$ hopOI, Nal <sup>r</sup>	This study
Pta D21E	Pta D20E, $\Delta$ hopM1, Nal <sup>r</sup>	This study
Pta D22E	Pta D22E, $\Delta$ hopM1-shcE, Nal <sup>r</sup>	This study
Pta D2E <sup>R</sup>	Pta $\Delta$ hopAE1, $\Delta$ hopW1, Nal <sup>r</sup>	This study
Pta D3E <sup>R</sup>	Pta D2E <sup>R</sup> , $\Delta$ hopM1, Nal <sup>r</sup>	This study
Pta D4E <sup>R</sup>	Pta D2E <sup>R</sup> , $\Delta$ hopM1-shcE, Nal <sup>r</sup>	This study
Pta D6E <sup>R</sup>	Pta D4E <sup>R</sup> , $\Delta$ hopOI-hopT1, Nal <sup>r</sup>	This study
Pta D7E <sup>R</sup>	Pta D6E <sup>R</sup> , $\Delta$ hopAZI, Nal <sup>r</sup>	This study
Plasmids		
pHSG396	a pUC type of cloning vector, Cm <sup>r</sup>	TaKaRa
pK18mobsacB	Small mobilisable vector, sucrose-sensitive ( <i>sacB</i> ); Km <sup>r</sup>	Schäfer et al. (1994)
pK18mobsacBN	NotI site inserted between PstI and HindIII site of MCS in pK18; Km <sup>r</sup>	Kashihara et al. (2022)
$\Delta$ hrcC	$\Delta$ Pta6605_RS21955 fragment-containing pK18, Km <sup>r</sup>	Kashihara et al. (2022)
$\Delta$ avrE1	$\Delta$ Pta6605_RS22015 fragment-containing pK18, Km <sup>r</sup>	Kashihara et al. (2022)
$\Delta$ avrPto4	$\Delta$ Pta6605_RS26865 fragment-containing pK18, Km <sup>r</sup>	Kashihara et al. (2022)
Pta $\Delta$ avrPtoB	$\Delta$ Pta6605_RS12680 fragment-containing pK18, Km <sup>r</sup>	Kashihara et al. (2022)
$\Delta$ hopAE1	$\Delta$ Pta6605_RS04955 fragment-containing pK18, Km <sup>r</sup>	Kashihara et al. (2022)
$\Delta$ hopAG1 $\Delta$ hopAH1 $\Delta$ hopAl1	$\Delta$ RS0109770 (old Acc.num.), $\Delta$ Pta6605_RS24195, $\Delta$ Pta6605_RS24190 fragment-containing pK18, Km <sup>r</sup>	Kashihara et al. (2022)
$\Delta$ hopAH2	$\Delta$ Pta6605_RS11715 fragment-containing pK18, Km <sup>r</sup>	Kashihara et al. (2022)
$\Delta$ hopAR1	$\Delta$ Pta6605_RS26885 fragment-containing pK18, Km <sup>r</sup>	Kashihara et al. (2022)
$\Delta$ hopAZI	$\Delta$ Pta6605_RS18960 fragment-containing pK18, Km <sup>r</sup>	Kashihara et al. (2022)
$\Delta$ hopBD1	$\Delta$ Pta6605_RS13890 fragment-containing pK18, Km <sup>r</sup>	Kashihara et al. (2022)
$\Delta$ hopE1	$\Delta$ Pta6605_RS18765 fragment-containing pK18, Km <sup>r</sup>	Kashihara et al. (2022)
Pta $\Delta$ hopF1	$\Delta$ Pta6605_RS20695 fragment-containing pK18, Km <sup>r</sup>	This study
Pta $\Delta$ hopI1	$\Delta$ Pta6605_RS04760 fragment-containing pK18, Km <sup>r</sup>	Kashihara et al. (2022)
$\Delta$ hopM1 $\Delta$ shcE	$\Delta$ Pta6605_RS22025, $\Delta$ Pta6605_RS22020 fragment-containing pK18, Km <sup>r</sup>	Kashihara et al. (2022)
$\Delta$ hopOI $\Delta$ hopT1	$\Delta$ Pta6605_RS20735, $\Delta$ Pta6605_RS20740 fragment-containing pK18, Km <sup>r</sup>	Kashihara et al. (2022)
$\Delta$ hopR1	$\Delta$ Pta6605_RS00920 fragment-containing pK18, Km <sup>r</sup>	Kashihara et al. (2022)
P $\Delta$ hopV1	$\Delta$ Pta6605_RS12945 fragment-containing pK18, Km <sup>r</sup>	Kashihara et al. (2022)
$\Delta$ hopW1	$\Delta$ Pta6605_RS13905 fragment-containing pK18, Km <sup>r</sup>	Kashihara et al. (2022)
$\Delta$ hopX1	$\Delta$ Pta6605_RS28265 fragment-containing pK18, Km <sup>r</sup>	Kashihara et al. (2022)

Note: Seven-digit annotation and five-digit annotation indicates the database source for Pta 6605. The accession number indicates the gene number in the Pseudomonas Genome Database.

Abbreviations: Cm<sup>r</sup>, chloramphenicol resistant; Km<sup>r</sup>, kanamycin resistant; Nal<sup>r</sup>, nalidixic acid resistant.



**FIGURE 1** | Disease development of *Pseudomonas syringae* pv. *tabaci* (Pta) 6605 single-locus  $\Delta$ T3E mutants on *Nicotiana benthamiana* by flood assay inoculation. (a) Pta suspensions were adjusted to optical density (OD)<sub>600</sub> = 0.002 and inoculated into 2-week-old *N. benthamiana* by the flood assay. Disease development was observed at 6 days post-inoculation (dpi; bar = 1 cm). Mock-treated (water), Pta wild type (WT), and Pta  $\Delta$ *hrcC* were used as controls. Three independent experiments were conducted with two independent individuals ( $n = 6$ ), and similar results were obtained. (b) The progression of the disease is divided into three levels (1, 2, and 3), and the percentage of each level is illustrated on the figure.  $n$  indicates the number of individuals used.

exhibited disease severity that was not significantly different from that of the Pta  $\Delta$ *hrcC* mutant, which lacks a functional T3SS (Figure 2a,b). Additionally, bacterial populations were assessed at 3 dpi using the flood assay (Figure 2c). Consistent with the suppression of disease symptoms, bacterial growth measured at 3 dpi was lower in Pta D18E and Pta D22E than in Pta WT (Figure 2c). In comparison with the Pta  $\Delta$ *hrcC* mutant, no significant difference in bacterial population was found between Pta D18E and Pta D20E, whereas bacterial growth was significantly greater in Pta D21E and Pta D22E than in Pta  $\Delta$ *hrcC* (Figure 2c).

The effectors deleted from Pta D14E to Pta D18E follow the order *hopAR1*, *hopF1*, *hopAZ1*, *hopW1*, and *hopAE1*. In Pta D20E, Pta D21E, and Pta D22E, the deleted effectors were *hopT1-hopO1*, *hopM1*, and *shcE*, respectively (Table 1). The *shcE* gene functions as a chaperone for AvrE1, and its secretion is impaired in the absence of *shcE* (Kvitko et al. 2009; Jayaraman et al. 2020). Because no symptom development was observed in Pta D22E (Figure 2b), these results suggest that at least the 22 T3Es deleted in this study play a major role in virulence as T3Es.

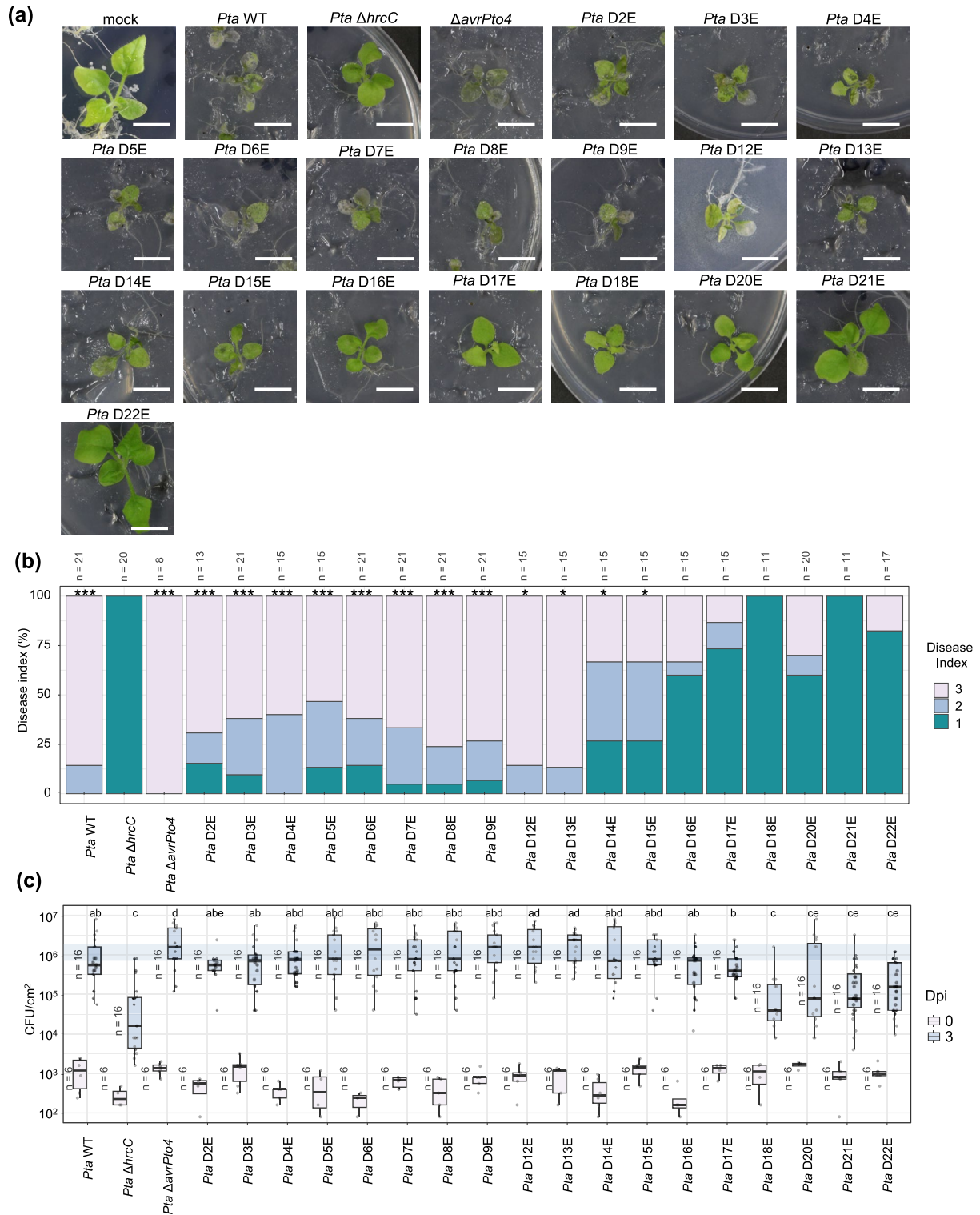


**FIGURE 2** | Prestomatal infection test reveals the role of type III effectors (T3Es) in disease development of *Pseudomonas syringae* pv. *tabaci* (*Pta*) DxE mutants. (a) *Pta* strains ( $OD_{600} = 0.002$ ) were inoculated into 2-week-old *Nicotiana benthamiana* through the flood assay. Disease development was observed at 6 days post-inoculation (dpi) (bar = 1 cm). Mock-treated (water), *Pta* WT, and *Pta*  $\Delta$ *hrcC* were used as controls. Three independent experiments were conducted with three independent individuals. (b) Disease severity was categorised into three levels as in Figure 1, with percentages shown. *n* indicates the total number of biological replicates. Statistical analyses were performed using Pearson's chi-square test comparing *Pta*  $\Delta$ *hrcC* with each strain, followed by Bonferroni correction (\* $p < 0.05$ , \*\*\* $p < 0.001$ ). (c) Bacterial populations in *N. benthamiana* leaves at 0 and 3 dpi. The two independent results were combined and illustrated in a boxplot. Boxes show upper and lower quartiles of the data, and black lines represent the medians. Each dot represents raw data. *n* indicates the total number of biological replicates. Different letters indicate statistically significant differences between groups (Kruskal-Wallis test followed by Dunn's multiple comparisons test with Benjamini-Hochberg correction,  $p < 0.05$ ).

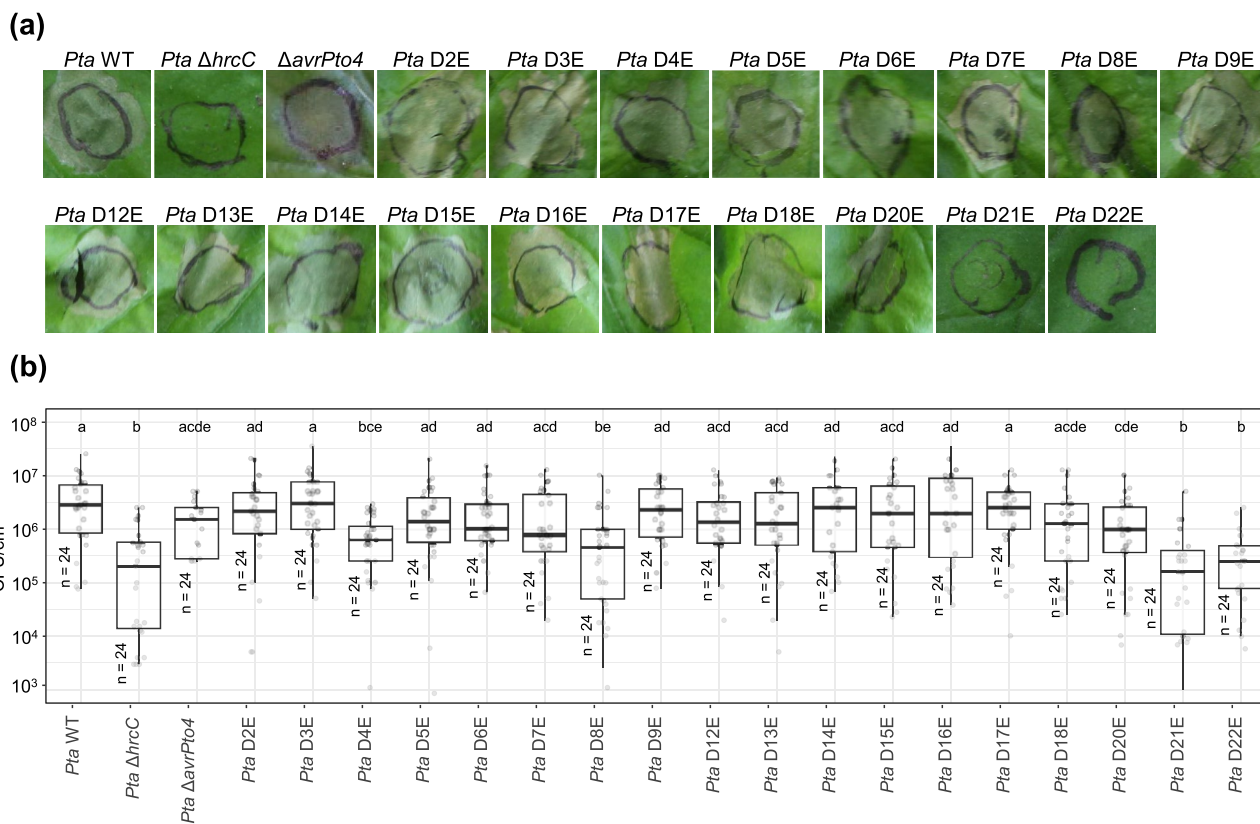


**FIGURE 3** | Post-stomatal infection test reveals type III effector (T3E)-dependent tissue colonisation in the *Pseudomonas syringae* pv. *tabaci* (*Pta*) DxE mutants. (a) *Pta* suspensions were adjusted to  $OD_{600} = 0.02$  and inoculated into 4- to 5-week-old *Nicotiana benthamiana* by the syringe infiltration method. Disease development was observed at 6 days post-inoculation (dpi). (b) Bacterial population tests on *N. benthamiana*. Plants were inoculated by infiltration assay, and bacterial populations were measured at 3 dpi. The results of three independent experiments were combined and are illustrated in the boxplot. Boxes show upper and lower quartiles of the data, and black lines represent the medians. Each dot represents a raw data point. *n* indicates the total number of biological replicates of plants used in the three independent experiments. Different letters indicate statistically significant differences between groups (Kruskal–Wallis test followed by Dunn's multiple comparisons test with Benjamini–Hochberg correction,  $p < 0.05$ ).

## 2.4 | *Pta* D21E and *Pta* D22E Suppress Cell Death Symptoms

Considering that *Pta* D14E to *Pta* D22E exhibited reduced symptom development, we investigated symptom development and bacterial populations by using an infiltration assay to determine whether the reduced virulence of the *Pta* DxE mutants is responsible for this outcome. We examined the effect of inoculum concentration during infiltration. Contrary to our expectation, a significant difference in bacterial growth between the *Pta* WT and *Pta*  $\Delta$ *hrcC* mutant was observed only at an inoculum concentration of  $OD_{600} = 0.02$  at 3 dpi (Figure S4). By contrast, no significant difference in bacterial population was detected between these strains at  $OD_{600} = 0.002$  at 6 dpi. Based on these findings, we evaluated bacterial growth in the *Pta* DxE mutants using an inoculum concentration of  $OD_{600} = 0.02$ . Infiltration assay results indicated that the cell death symptoms induced by *Pta* D14E to *Pta* D20E were slightly weak and delayed, but symptoms similar to those induced by *Pta* WT eventually developed (Figure 3a, Figure S5). Furthermore, differences in bacterial populations were observed in *Pta* D14E to *Pta* D20E compared with *Pta*  $\Delta$ *hrcC* (Figure 3b). These findings suggest that the *Pta* D14E to *Pta* D20E mutants retained the ability to cause cell

death symptoms when injected into plant tissue. However, in the plants inoculated with *Pta* D21E and *Pta* D22E, cell death symptoms were markedly decreased to a level comparable to that in the plants inoculated with the *Pta*  $\Delta$ *hrcC* mutant (Figure 3a and Figure S5). No significant differences in bacterial populations were found between the *Pta*  $\Delta$ *hrcC* mutant and the *Pta* D4E, *Pta* D8E, *Pta* D21E, and *Pta* D22E mutants (Figure 3b). *Pta* D20E contains AvrE1 and HopM1, *Pta* D21E contains only AvrE1, and *Pta* D22E lacks all predicted T3Es functions. These results indicate that AvrE1 and HopM1 of *Pta* 6605 play important roles in symptom expression after invasion of plant tissues. These results suggest that some combination of the T3Es (HopAZ1, HopW1, HopAE1, HopT1, and HopO1) possibly contributes to invasion through natural openings.

## 2.5 | Construction and Virulence Assay of Reverse-Complemented *Pta* DxE (*Pta* DxE<sup>R</sup>) Mutants Lacking Seven T3Es

Flood assay results suggested that at least seven T3Es (HopAZ1, HopW1, HopAE1, HopT1, HopO1, HopM1, and AvrE1) are required for *Pta* 6605 invasion through

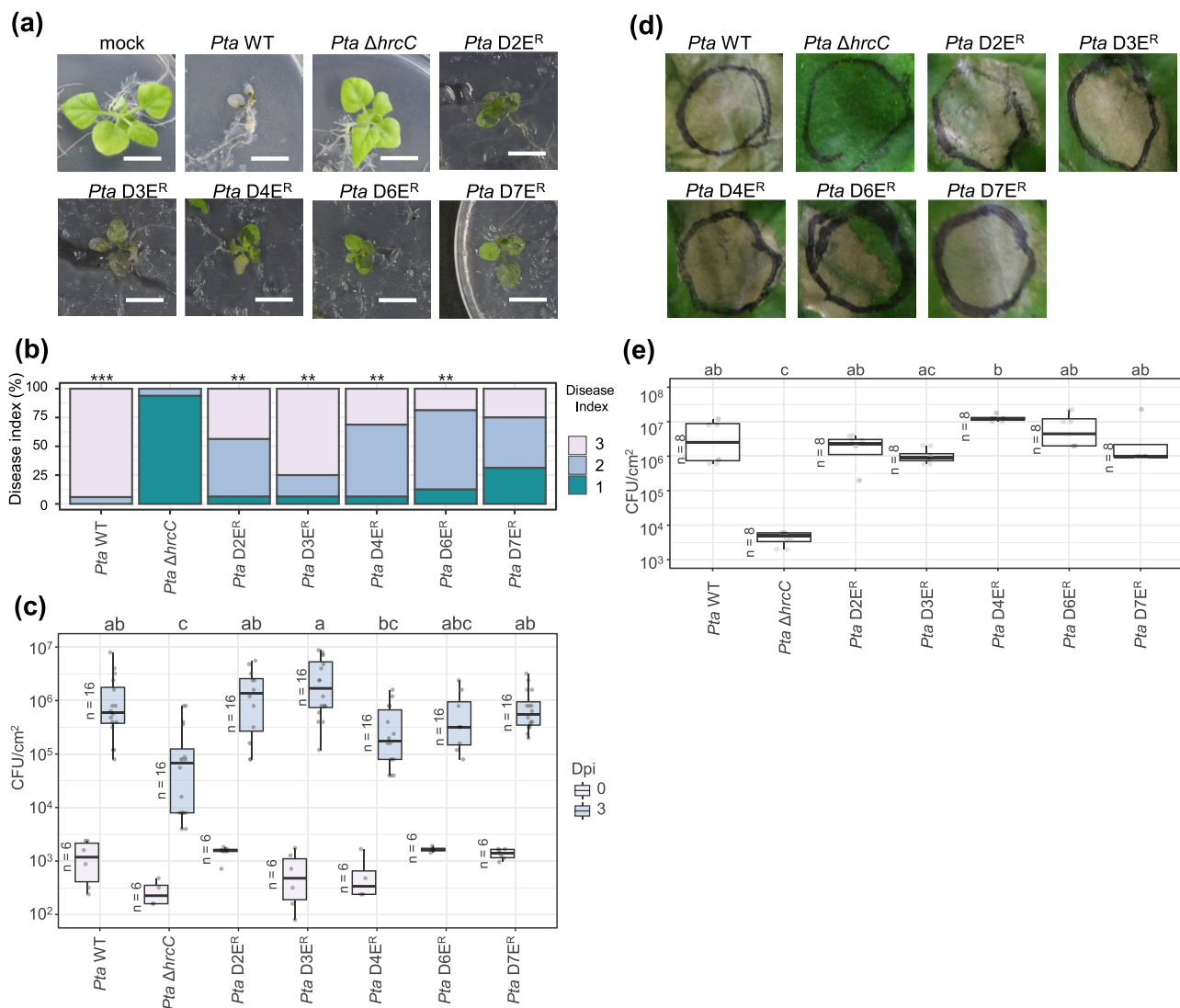


**FIGURE 4** | Validation of the contribution of seven type III effectors (T3Es) to virulence using *Pseudomonas syringae* pv. *tabaci* (*Pta*) DxE<sup>R</sup> under flood and infiltration assay conditions. (a) *Pta* suspensions were adjusted to OD<sub>600</sub> = 0.02 and inoculated into 2-week-old *Nicotiana benthamiana* by the flood assay method. Disease development was observed at 6 days post-inoculation (dpi) (bar = 1 cm). Mock-treated (water) plants, *Pta* wild type (WT)-inoculated, and *Pta*  $\Delta hrcC$ -inoculated plants were used as controls. Three independent experiments were conducted with three independent individuals ( $n = 9$ ). (b) The progression of the disease is divided into three levels as mentioned in Figure 1, and the percentage of each level is illustrated on the figure. Four independent experiments were conducted with four independent individuals ( $n = 16$ ). (c) Bacterial populations in *N. benthamiana* leaves at 0 and 3 dpi in flood assay. The two independent results were combined and illustrated in a boxplot. Each dot represents raw data.  $n$  indicates the total individuals. Different letters indicate statistically significant differences between groups (Kruskal–Wallis test followed by Dunn’s multiple comparisons test with Benjamini–Hochberg correction,  $p < 0.05$ ). (d) *Pta* suspensions were adjusted to OD<sub>600</sub> = 0.02 and inoculated into 4- to 5-week-old *N. benthamiana* by the infiltration method. Disease development was observed at 6 dpi. *Pta* WT and *Pta*  $\Delta hrcC$  were used as controls. Three independent experiments were conducted with three independent individuals ( $n = 9$ ). (e) Bacterial populations in *N. benthamiana* leaves at 3 dpi by the infiltration method. *Pta* suspensions were adjusted to OD<sub>600</sub> = 0.02. The three independent results were combined and illustrated in a boxplot. Each dot represents raw data.  $n$  indicates the total individuals. Different letters indicate statistically significant differences between groups (Kruskal–Wallis test followed by Dunn’s multiple comparisons test with Benjamini–Hochberg correction,  $p < 0.05$ ).

natural openings in *N. benthamiana* (Figure 2a). We examined whether these seven T3Es play a central role in the virulence of *Pta* to *N. benthamiana*. To assess their contributions, we sequentially deleted each of these effectors from the *Pta*  $\Delta hopAE1$  mutant, generating a series of mutant strains (*Pta* DxE reverse: *Pta* DxE<sup>R</sup>). Among these effectors, *Pta* possesses two T3Es belonging to the HopW1 superfamily: HopAE1 and HopW1. To investigate their roles, we generated a double mutant lacking *hopAE1* and *hopW1* and assessed its effect

on symptom development (Table 1). With the double mutant, the proportion of class 1–2 disease index increased to approximately 50% (Figure 4b). These results suggest that these two T3Es contribute to early infection (Figure 4a). However, given their lack of difference in bacterial growth from *Pta* WT, poly-T3E deletion mutants putatively involved in invasion through the stomata were constructed based on no difference in these double mutants. Subsequently, their contribution to virulence was evaluated. The genes were deleted in the order of *hopW1*

(Pta D2E<sup>R</sup>), *hopM1* (Pta D3E<sup>R</sup>), *shcE* (Pta D4E<sup>R</sup>), *hopO1-hopT1* (Pta D6E<sup>R</sup>), and *hopAZ1* (Pta D7E<sup>R</sup>) (Table 1). We confirmed that the Pta DxER mutants exhibited *in vitro* growth (Figure S3) and swimming motility (Figure S6). We further examined symptom development and bacterial populations in the Pta DxER mutants. Flood assay results revealed no significant difference in symptom development between the Pta D7E<sup>R</sup> and Pta  $\Delta hrcC$  mutants (Figure 4a,b). By contrast, bacterial growth analysis in the flood assay revealed that all mutants significantly differed from the Pta  $\Delta hrcC$  mutant (Figure 4c).

When we examined cell death symptom development via infiltration assay, we observed that only the Pta D7E<sup>R</sup> mutant showed delayed cell death symptom onset at 6 dpi (Figure S7a). By contrast, no significant difference in bacterial growth was found between the Pta  $\Delta hrcC$  and Pta DxER mutants at 3 dpi (Figure 4e, Figure S7b). These results demonstrate that while the Pta D7E<sup>R</sup> mutant retains the ability to proliferate within plant tissues, its virulence is slightly reduced. Our findings suggest that some combination of these seven T3Es contributes to the virulence of Pta 6605 to *N. benthamiana*.

To determine whether the bacterial population at the time of infiltration merely reflected the initial inoculum or had multiplied within the plant, we quantified the bacterial population at 0 and 3 dpi. Results showed that the bacterial population increased from the initial inoculum at 0 dpi to approximately 10<sup>6</sup> CFU/cm<sup>2</sup> at 3 dpi (Figure S8). These findings indicate that the observed increase is due to active bacterial growth within the plant rather than simply maintaining the initial inoculum.

### 3 | Discussion

In this study, we established a model system composed of *N. benthamiana* and Pta 6605 to investigate the functions of effectors in host–pathogen interactions. Previous studies have identified a minimal T3E repertoire (AvrE1, HopM1, HopE1, AvrPtoB, HopG1, HopAA1-1, and HopAM1) required by Pto DC3000 to infect *N. benthamiana* (Kvitko et al. 2009; Cunnac et al. 2011). Similar to Pta 11528, Pta 6605 lacks *hopG1* and *hopAM1*, and *hopAA1-1* is nonfunctional because of the frameshift mutation caused by a single base insertion (Baltrus et al. 2011; Matsui et al. 2021). Considering those differences, we explored the key T3Es required in the Pta-mediated infection of *N. benthamiana* using a series of single-locus T3E mutants. Although most T3E-deficient strains did not exhibit a significant reduction in virulence, class 2 symptoms were observed in 10%–20% of the plants inoculated with  $\Delta avrE1$ ,  $\Delta avrPtoB$ ,  $\Delta hopR1$ ,  $\Delta hopT1-hopO1$ , and  $\Delta hopV1$  mutants, suggesting that even a single mutation in a T3E may have a minor effect on virulence (Figure 1). Thus, we generated poly-T3E deletion mutants to investigate differences in Pta 6605 virulence. We focused on two key effectors, AvrPto4 and AvrPtoB, which target the PTI complex in Pto DC3000 and influence bacterial proliferation during infection (Cohn and Martin 2005; Lin and Martin 2005; He et al. 2006). Consistent with findings in the Pto DC3000–tomato system (Lin and Martin 2005), where similar effectors are implicated in immune suppression, the Pta D2E mutant exhibited an approximately 20% higher ratio of class 1–2 disease index. This finding suggests

that AvrPto4 and AvrPtoB also contribute to the suppression of immune responses in Pta 6605.

By constructing a series of Pta poly-T3E-deficient mutants, we identified seven T3Es (HopAZ1, HopW1, HopAE1, HopT1, HopO1, HopM1, and AvrE1) as the minimum repertoire required for Pta 6605 to invade natural openings and infect *N. benthamiana*. Plants inoculated with Pta D14E to Pta D20E showed reduced disease symptom development associated with invasion through natural openings. However, cell death symptoms still developed upon infiltration inoculation (Figure 3, Figure S5). Thus, these T3Es possibly contribute to Pta 6605 invasion through natural openings. From the perspective of infection strategies, the distinct minimal effector repertoires of Pto DC3000 and Pta 6605 may be attributed to differences in their interactions with the host. For Pto DC3000, the absence of *hopQ1-1* is a prerequisite for infection of *N. benthamiana*, suggesting that Pto DC3000 exhibits a non-adapted interaction with its host (Wei et al. 2007). Pto DC3000 deploys a repertoire of 36 T3Es and secretes coronatine to facilitate stomatal entry and modulate host immunity (Melotto et al. 2024). Meanwhile, Pta 6605 adopts tobacco plants as its host and evades host recognition by glycosylation of its flagella (Taguchi et al. 2006). Pta secretes the nonspecific plant toxin tabtoxin, which has chlorosis-inducing activity (Bender et al. 1999). In contrast to Pto DC3000, Pta 6605 does not secrete coronatine. Thus, the mechanism by which it regulates stomata during the early stages of infection in the host plant remains unclear. Unlike  $\Delta hrcC$  mutant of Pto DC3000 and Pss B728a (Wei et al. 2007), the Pta 6605  $\Delta hrcC$  proliferates more readily in *N. benthamiana* upon inoculation (Figures S4 and S7). However, despite this increased growth, no typical disease symptoms develop, suggesting that Pta 6605  $\Delta hrcC$  deploys alternative virulence factors or may have molecular mechanisms to facilitate host colonisation. However, this remains speculative. Such infection strategies could underlie the distinctive T3E repertoire of Pta 6605. Indeed, transient expression of HopT1-1 and HopW1 from Pta 11528 suppresses Ca<sup>2+</sup> bursts, reactive oxygen species (ROS) bursts, and defence gene expression triggered by flg22 or chitin treatment (Gimenez-Ibanez et al. 2018). Therefore, in addition to sharing common effectors such as AvrE1, HopM1, and HopT1 with Pto DC3000, Pta 6605 may have evolved a repertoire that includes effectors that more effectively suppress plant immunity, thereby enabling efficient infection of *N. benthamiana*.

Pta D20E, which retains only two T3E genes along with their chaperone genes, *shcE-avrE1* and *shcM-hopM1*, caused disease symptoms in *N. benthamiana* when infiltrated (Figure 3, Figure S5). No symptom development was observed in plants inoculated with Pta D21E, indicating that these two T3Es play an important role in bacterial growth in plants. This finding is consistent with the results of previous analyses on Pto DC3000 (Roussin-Léveillé et al. 2022). The lack of *shcE* suppresses the function of AvrE1, as shown by the reduction in bacterial population to the same level as Pta D22E and Pta  $\Delta hrcC$  mutants in the infiltration inoculation (Figure 3b). AvrE1, a highly conserved T3E in plant-pathogenic bacteria, forms a water channel that facilitates bacterial proliferation (Nomura et al. 2023; Herold et al. 2024). HopM1 suppresses early PTI responses, such as ROS bursts and stomatal immunity, by degrading AtMIN7, a

crucial factor for cellular integrity (Nomura et al. 2006). HopM1 also degrades 14-3-3 proteins, weakening the plant immune system and suppressing PTI (Gampala et al. 2007; Lozano-Durán et al. 2014). Additionally, HopM1 contributes to water-soaking by causing stomatal closure in the Pto DC3000–*Arabidopsis* model system (Roussin-Léveillé et al. 2022). Based on the results of the inoculation of Pta D21E and Pta D22E (Figures 2 and 3), we investigated the effects of AvrE1 and HopM1 on virulence. Results showed that the loss of AvrE1 and HopM1 alone did not cause a dramatic decrease in virulence (Figure 4a). The effects of AvrE1 and HopM1 as virulence factors may be difficult to detect under the conditions of this study. For this reason, an evaluation system must be developed in the future to clarify the roles of individual T3Es. Conversely, the Pta D7E<sup>R</sup> mutant delayed symptom development (Figure 4b, Figure S7a), suggesting that AvrE1 and HopM1 play a significant role in the virulence of Pta 6605 to *N. benthamiana*.

The T3Es identified in this study, including HopAZ1, HopW1, HopAE1, HopT1, and HopO1, have been reported to be involved in regulating plant immunity. For instance, HopAZ1 from *Pseudomonas savastanoi* pv. *savastanoi* NCPPB3335 inhibits ROS production and callose deposition, thereby acting as a virulence factor in *Nicotiana tabacum* (Matas et al. 2014). Pta 6605 possesses two HopW1 family proteins. HopW1 reportedly disrupts the actin cytoskeleton and reduces vesicular transport in *Arabidopsis thaliana* (Kang et al. 2014). The molecular function of HopAE1 is unclear, but HopAE1 from Pss B728a induces cell death in *N. benthamiana* when transiently expressed, and this cell death is suppressed by virus-induced gene silencing of *EDS1* (Vinatzer et al. 2006). The amino acid sequence identity between HopAE1 of Pss B728a and HopAE1 of Pta 6605 is 94%. Pta HopAE1 also induces cell death by transient expression assay (Figure S1), suggesting that a common mechanism exists between the two (Vinatzer et al. 2006). HopO1 and HopT1 are tandemly present in the genome and were deleted simultaneously; thus, whether HopO1 or HopT1 is more important remains unclear. HopT1 is required for the pathogenicity of Pto DC3000, and it exerts its effects by targeting AGO1, an important component of the plant's immune system (Thiébeauld et al. 2023). HopO1 is a key effector used by Pto DC3000 to manipulate plasmodesmatal function. HopO1 interacts with proteins such as PDLP5 and PDLP7, which localise to the plasmodesmata, contributing to bacterial virulence by altering plasmodesmatal permeability (Aung et al. 2020). Based on their high sequence identity with HopT1-1 (98%) and HopO1-1 (99%) from Pto DC3000, HopT1 and HopO1 of Pta 6605 are predicted to have similar molecular functions.

These individual T3Es possibly contribute to plant immunity suppression during the early stages of invasion through the stomata; however, further analyses are required. In the present study, we identified only one possible combination of essential T3Es (consisting of HopAZ1, HopW1, HopAE1, HopT1, HopO1, HopM1, and AvrE1) for successful stomatal infection, but alternative combinations may exist. The molecular functions of the T3Es and their potential interactions still need to be explored. Regarding the discrepancy between the disease index and bacterial growth in the flood assay, the assay was conducted under conditions highly favourable for bacterial proliferation (Figure 2b,c). Moreover, many leaves

were severely damaged at 3 dpi, preventing surface sterilisation; thus, bacterial counts possibly include both epiphytic and endophytic populations. A key limitation of our study is the lack of complementation tests to confirm virulence restoration by T3Es in Pta 6605. Although efficient transformation systems have been established for model strains such as Pto DC3000 (Cunnac et al. 2011; Wei et al. 2018), complementation in Pta 6605 is challenging because transformation can only be achieved via conjugation. Developing more efficient transformation methods for Pta 6605 will be crucial for future detailed functional analyses of its T3Es.

In summary, we have constructed several T3E deletion mutants as a basis for understanding the virulence of Pta 6605. The minimal T3E repertoire required by Pta 6605 to infect *N. benthamiana* differs from that required by Pto DC3000. This finding, which demonstrates that Pta 6605 can achieve virulence with a T3E repertoire distinct from that of Pto DC3000, provides novel insights into the evolution and diversification of infection strategies in plant-pathogenic bacteria. However, many T3Es appear to play minor roles in virulence; thus, further investigation is needed to elucidate the detailed mechanisms of these effectors as virulence factors.

## 4 | Experimental Procedures

### 4.1 | Plant and Bacterial Strains

*Nicotiana benthamiana* was grown at 28°C under 16 h light/8 h dark conditions. In the flood assay, sterilised *N. benthamiana* seeds were sown on Murashige and Skooge (MS) 1% sucrose 0.8% agar plates. At 10 days after sowing, the plants were transferred to MS 0.05% sucrose 0.8% agar plates supplemented with MS vitamins (3 mg/L thiamine hydrochloride, 5 mL/L nicotinic acid, and 0.5 mg/L pyridoxine hydrochloride) for inoculation and then cultured for 2 or 3 days. In the infiltration assay, the plants were planted in a 1:1 mixture of vermiculite and Supermix A (Sakatanotane) soil and allowed to grow for 4 or 5 weeks. *Escherichia coli* DH5a and S17-1 strains were grown at 37°C in Luria Bertani (LB) medium with appropriate antibiotics. Although the phytopathogen's scientific name is *Pseudomonas amygdali* pv. *tabaci*, it is commonly referred to as *P. syringae* pv. *tabaci* (Pta) in the literature. Pta 6605 was cultured at 27°C on 1.5% agar plates containing 50 µg/mL nalidixic acid (final concentration) in King's B (KB) medium.

### 4.2 | Generation of Poly-T3E Deletion Mutants of Pta 6605

Poly-T3E deletion mutants of Pta 6605 were constructed using the pK18*mobsacBN*- $\Delta$ T3E vector series as previously described by Kashihara et al. (2022). For example, the *hopF1* deletion mutant was constructed through PCR amplification of the upstream and downstream regions of *hopF1*. The primer sets employed (Table S1, S10) were designed based on the Pta 6605 genome sequence and inserted into the EcoRI site of pK18*mobsacBN* (Kashihara et al. 2022) using the IN-Fusion HD Cloning kit (TaKaRa). The sequence of pK18*mobsacBN*- $\Delta$ *hopF1* was confirmed by Sanger sequencing and used to generate poly-T3E

mutants. The poly-T3E deletion mutants were generated by conjugation with *E. coli* S17-1 (Schäfer et al. 1994) and homologous recombination by incubation on KB agar plates containing 10% sucrose and 50 µg/mL nalidixic acid. The prepared mutants were used in subsequent experiments after confirming the deletion of the target region by PCR and verifying motility. The Pta T3E-deletion mutant series generated in this study is summarised in Table 1.

### 4.3 | Inoculation Test

The inoculation test was conducted using two types of inoculation methods, flood and infiltration assays. The flood assay was performed as previously described (Ishiga et al. 2011; Tumewu et al. 2020). The bacterial suspension was adjusted to an optical density (OD)<sub>600</sub> of 0.002, and Silwet L-77 (Biomedical Sciences) was added to a final concentration of 0.025%. *N. benthamiana* was then flooded with the bacterial suspension, allowed to air dry for 15 min in a clean bench, and then incubated at 22°C under 16 h light/8 h dark conditions. The disease symptoms were monitored at 3, 6, and 10 dpi.

In the infiltration assay, the precultured bacterial suspension was collected and suspended in 10 mM MgCl<sub>2</sub> to OD<sub>600</sub> = 0.2 or 0.02, or 0.002. The bacterial suspension was then inoculated on the abaxial leaf using a needleless syringe. Subsequently, the plants were incubated at 22°C under 16 h light/8 h dark conditions. The cell death symptoms were observed at 6 and 14 dpi. After inoculation, the bacterial population was measured as colony-forming units on KB plates containing Nal.

### 4.4 | Other Methods

Details of agroinfiltration assays, trypan blue staining, in vitro bacterial growth assay, motility assay, vector construction for transient expression assay, and bacterial strains and plasmids used for supplementary experiments are provided in S9.

### 4.5 | Statistical Analysis

Statistical analyses were performed using Pearson's chi-square test with Bonferroni correction, the Kruskal–Wallis test followed by Dunn's multiple comparisons test with the Benjamini–Hochberg method, and the Welch's *t* test. All analyses were performed using R software (v. 4.4.1; <https://www.r-project.org/>) and RStudio (v. 2024.04.02 + 764; <https://posit.co/download/rstudio-desktop/>).

### Acknowledgements

The authors would like to thank the Leaf Tobacco Research Laboratory of Japan Tobacco Inc. for providing Pta 6605. We also thank the National BioResource Project (NIG, Japan): *E. coli* for providing the *E. coli* S17-1 strain. We thank Dr Tsuyoshi Nakagawa (Shimane University) for providing pGWB Gateway binary vectors. This work was supported in part by Grants-in-Aid for Scientific Research (H.M., 22K05653; Y.I., 23K23613) from the Ministry of Education, Culture, Sports, Science and Technology of Japan.

### Conflicts of Interest

The authors declare no conflicts of interest.

### Data Availability Statement

The data that support the findings of this study are available from the corresponding author upon reasonable request.

### References

- Aung, K., P. Kim, Z. Li, et al. 2020. "Pathogenic Bacteria Target Plant Plasmodesmata to Colonize and Invade Surrounding Tissues." *Plant Cell* 32: 595–611.
- Baltrus, D. A., M. T. Nishimura, A. Romanchuk, et al. 2011. "Dynamic Evolution of Pathogenicity Revealed by Sequencing and Comparative Genomics of 19 *Pseudomonas syringae* Isolates." *PLoS Pathogens* 7: e1002132.
- Bender, C. L., F. Alarcón-Chaidez, and D. C. Gross. 1999. "*Pseudomonas syringae* Phytotoxins: Mode of Action, Regulation, and Biosynthesis by Peptide and Polyketide Synthetases." *Microbiology and Molecular Biology Reviews* 63: 266–292.
- Büttner, D. 2016. "Behind the Lines – Actions of Bacterial Type III Effector Proteins in Plant Cells." *FEMS Microbiology Reviews* 40: 894–937.
- Chakravarthy, S., J. N. Worley, A. Montes-Rodriguez, and A. Collmer. 2018. "*Pseudomonas syringae* pv. *tomato* DC3000 Polymutants Deploying Coronatine and Two Type III Effectors Produce Quantifiable Chlorotic Spots From Individual Bacterial Colonies in *Nicotiana benthamiana* Leaves." *Molecular Plant Pathology* 19: 935–947.
- Coburn, B., I. Sekirov, and B. B. Finlay. 2007. "Type III Secretion Systems and Disease." *Clinical Microbiology Reviews* 20: 535–549.
- Cohn, J. R., and G. B. Martin. 2005. "*Pseudomonas syringae* pv. *tomato* Type III Effectors AvrPto and AvrPtoB Promote Ethylene-Dependent Cell Death in Tomato." *Plant Journal* 44: 139–154.
- Cunnac, S., S. Chakravarthy, B. H. Kvitko, A. B. Russell, G. B. Martin, and A. Collmer. 2011. "Genetic Disassembly and Combinatorial Reassembly Identify a Minimal Functional Repertoire of Type III Effectors in *Pseudomonas syringae*." *Proceedings of the National Academy of Sciences of the United States of America* 108: 2975–2980.
- Dillon, M. M., R. N. D. Almeida, B. Laflamme, et al. 2019. "Molecular Evolution of *Pseudomonas syringae* Type III Secreted Effector Proteins." *Frontiers in Plant Science* 10: 418.
- Gampala, S. S., T.-W. Kim, J.-X. He, et al. 2007. "An Essential Role for 14–3-3 Proteins in Brassinosteroid Signal Transduction in *Arabidopsis*." *Developmental Cell* 13: 177–189.
- Gimenez-Ibanez, S., D. R. Hann, J. H. Chang, C. Segonzac, T. Boller, and J. P. Rathjen. 2018. "Differential Suppression of *Nicotiana benthamiana* Innate Immune Responses by Transiently Expressed *Pseudomonas syringae* Type III Effectors." *Frontiers in Plant Science* 9: 688.
- He, P., L. Shan, N.-C. Lin, et al. 2006. "Specific Bacterial Suppressors of MAMP Signaling Upstream of MAPKKK in *Arabidopsis* Innate Immunity." *Cell* 125: 563–575.
- Herold, L., S. Choi, S. Y. He, and C. Zipfel. 2024. "The Conserved AvrE Family of Bacterial Effectors: Functions and Targets During Pathogenesis." *Trends in Microbiology* 33: 184–193.
- Ichinose, Y., R. Shimizu, Y. Ikeda, et al. 2003. "Need for Flagella for Complete Virulence of *Pseudomonas syringae* pv. *tabaci*: Genetic Analysis With Flagella-Defective Mutants Δ*fliC* and Δ*fliD* in Host Tobacco Plants." *Journal of General Plant Pathology* 69: 244–249.
- Ishiga, Y., T. Ishiga, S. R. Uppalapati, and K. S. Mysore. 2011. "Arabidopsis Seedling Flood-Inoculation Technique: A Rapid and Reliable Assay for Studying Plant–Bacterial Interactions." *Plant Methods* 7: 32.

- Jayaraman, J., M. Yoon, E. R. Applegate, E. A. Stroud, and M. D. Templeton. 2020. "AvrE1 and HopR1 From *Pseudomonas syringae* pv. *actinidiae* Are Additively Required for Full Virulence on Kiwifruit." *Molecular Plant Pathology* 21: 1467–1480.
- Kang, Y., J. Jelenska, N. M. Cecchini, et al. 2014. "HopW1 From *Pseudomonas syringae* Disrupts the Actin Cytoskeleton to Promote Virulence in *Arabidopsis*." *PLoS Pathogens* 10: e1004232.
- Kashihara, S., T. Nishimura, Y. Noutoshi, et al. 2022. "HopAZ1, a Type III Effector of *Pseudomonas amygdali* pv. *tabaci*, Induces a Hypersensitive Response in Tobacco Wildfire-Resistant *Nicotiana tabacum* 'N509'." *Molecular Plant Pathology* 23: 885–894.
- Khan, M., D. Seto, R. Subramaniam, and D. Desveaux. 2018. "Oh, the Places They'll Go! A Survey of Phytopathogen Effectors and Their Host Targets." *Plant Journal* 93: 651–663.
- Kvitko, B. H., D. H. Park, A. C. Velásquez, et al. 2009. "Deletions in the Repertoire of *Pseudomonas syringae* pv. *tomato* DC3000 Type III Secretion Effector Genes Reveal Functional Overlap Among Effectors." *PLoS Pathogens* 5: e1000388.
- Lin, N.-C., and G. B. Martin. 2005. "An *avrPto/avrPtoB* Mutant of *Pseudomonas syringae* pv. *tomato* DC3000 Does Not Elicit Pto-Mediated Resistance and Is Less Virulent on Tomato." *Molecular Plant-Microbe Interactions* 18: 43–51.
- Lozano-Durán, R., G. Bourdais, S. Y. He, and S. Robatzek. 2014. "The Bacterial Effector HopM1 Suppresses PAMP-Triggered Oxidative Burst and Stomatal Immunity." *New Phytologist* 202: 259–269.
- Marutani, M., F. Taguchi, R. Shimizu, et al. 2005. "Flagellin from *Pseudomonas syringae* pv. *tabaci* Induced hrp-independent HR in Tomato." *Journal of General Plant Pathology* 71: 289–295.
- Matas, I. M., M. P. Castañeda-Ojeda, I. M. Aragón, et al. 2014. "Translocation and Functional Analysis of *Pseudomonas savastanoi* pv. *savastanoi* NCPPB 3335 Type III Secretion System Effectors Reveals Two Novel Effector Families of the *Pseudomonas syringae* Complex." *Molecular Plant-Microbe Interactions* 27: 424–436.
- Matsui, H., T. Nishimura, S. Asai, et al. 2021. "Complete Genome Sequence of *Pseudomonas amygdali* pv. *tabaci* Strain 6605, a Causal Agent of Tobacco Wildfire Disease." *Microbiology Resource Announcements* 10: e0040521.
- Melotto, M., B. Fochs, Z. Jaramillo, and O. Rodrigues. 2024. "Fighting for Survival at the Stomatal Gate." *Annual Review of Plant Biology* 75: 551–577.
- Nomura, K., F. Andreatza, J. Cheng, K. Dong, P. Zhou, and S. Y. He. 2023. "Bacterial Pathogens Deliver Water- and Solute-Permeable Channels to Plant Cells." *Nature* 621: 586–591.
- Nomura, K., S. DebRoy, Y. H. Lee, N. Pumplin, J. Jones, and S. Y. He. 2006. "A Bacterial Virulence Protein Suppresses Host Innate Immunity to Cause Plant Disease." *Science* 313: 220–223.
- Oh, H.-S., D. H. Park, and A. Collmer. 2010. "Components of the *Pseudomonas syringae* Type III Secretion System Can Suppress and May Elicit Plant Innate Immunity." *Molecular Plant-Microbe Interactions* 23: 727–739.
- Roussin-Léveillé, C., G. Lajeunesse, M. St-Amand, et al. 2022. "Evolutionarily Conserved Bacterial Effectors Hijack Abscisic Acid Signaling to Induce an Aqueous Environment in the Apoplast." *Cell Host & Microbe* 30: 489–501.e4.
- Schäfer, A., A. Tauch, W. Jäger, J. Kalinowski, G. Thierbach, and A. Pühler. 1994. "Small Mobilizable Multi-Purpose Cloning Vectors Derived From the *Escherichia coli* Plasmids pK18 and pK19: Selection of Defined Deletions in the Chromosome of *Corynebacterium glutamicum*." *Gene* 145: 69–73.
- Shimizu, R., F. Taguchi, M. Marutani, et al. 2003. "The *ΔfliD* mutant of *Pseudomonas syringae* pv. *tabaci*, Which Secretes Flagellin Monomers, Induces a Strong Hypersensitive Reaction (HR) in Non-host Tomato Cells." *Molecular Genetics and Genomics* 269: 21–30.
- Speth, E. B., Y. N. Lee, and S. Y. He. 2007. "Pathogen Virulence Factors as Molecular Probes of Basic Plant Cellular Functions." *Current Opinion in Plant Biology* 10: 580–586.
- Studholme, D. J., S. Ibanez, D. MacLean, J. L. Dangel, J. H. Chang, and J. P. Rathjen. 2009. "A Draft Genome Sequence and Functional Screen Reveals the Repertoire of Type III Secreted Proteins of *Pseudomonas syringae* Pathovar *tabaci* 11528." *BMC Genomics* 10: 395.
- Taguchi, F., K. Takeuchi, E. Katoh, et al. 2006. "Identification of Glycosylation Genes and Glycosylated Amino Acids of Flagellin in *Pseudomonas syringae* pv. *Ttabaci*." *Cellular Microbiology* 8: 923–938.
- Thiébeauld, O., M. Charvin, M. Singla-Rastogi, et al. 2023. "A Bacterial Effector Directly Targets *Arabidopsis* Argonaute 1 to Suppress Pattern-Triggered Immunity and Cause Disease." *bioRxiv* [Preprint]. <https://doi.org/10.1101/215590>.
- Tumewu, S. A., H. Matsui, M. Yamamoto, Y. Noutoshi, K. Toyoda, and Y. Ichinose. 2020. "Requirement of  $\gamma$ -Aminobutyric Acid Chemotaxis for Virulence of *Pseudomonas syringae* pv. *tabaci* 6605." *Microbes and Environments* 35: ME20114.
- Vinatzer, B. A., G. M. Teitzel, M.-W. Lee, et al. 2006. "The Type III Effector Repertoire of *Pseudomonas syringae* pv. *syringae* B728a and Its Role in Survival and Disease on Host and Non-Host Plants." *Molecular Microbiology* 62: 26–44.
- Wei, C.-F., B. H. Kvitko, R. Shimizu, et al. 2007. "A *Pseudomonas syringae* pv. *tomato* DC3000 Mutant Lacking the Type III Effector HopQ1-1 Is Able to Cause Disease in the Model Plant *Nicotiana benthamiana*." *Plant Journal* 51: 32–46.
- Wei, H.-L., S. Chakravarthy, J. Mathieu, et al. 2015. "Pseudomonas syringae pv. *tomato* DC3000 Type III Secretion Effector Polymutants Reveal an Interplay Between HopAD1 and AvrPtoB." *Cell Host & Microbe* 17: 752–762.
- Wei, H.-L., W. Zhang, and A. Collmer. 2018. "Modular Study of the Type III Effector Repertoire in *Pseudomonas syringae* pv. *tomato* DC3000 Reveals a Matrix of Effector Interplay in Pathogenesis." *Cell Reports* 23: 1630–1638.
- Xin, X.-F., B. Kvitko, and S. Y. He. 2018. "Pseudomonas syringae: What It Takes to Be a Pathogen." *Nature Reviews Microbiology* 16: 316–328.
- Xin, X.-F., K. Nomura, K. Aung, et al. 2016. "Bacteria Establish an Aqueous Living Space in Plants Crucial for Virulence." *Nature* 539: 524–529.
- Yang, L., P. J. P. L. Teixeira, S. Biswas, et al. 2017. "Pseudomonas syringae Type III Effector HopBB1 Promotes Host Transcriptional Repressor Degradation to Regulate Phytohormone Responses and Virulence." *Cell Host & Microbe* 21: 156–168.
- Zhou, J.-M., and J. Chai. 2008. "Plant-Pathogenic Bacterial Type III Effectors Subdue Host Responses." *Current Opinion in Microbiology* 11: 179–185.

### Supporting Information

Additional supporting information can be found online in the Supporting Information section.